JMEPEG (2010) 19:955–962
DOI: 10.1007/s11665-009-9582-8

1059-9495/$19.00

Investigations on the Effects of the Tool Material, Geometry, and Tilt Angle on Friction Stir Welding of Pure Titanium

K. Reshad Seighalani, M.K. Besharati Givi, A.M. Nasiri, and P. Bahemmat

(Submitted October 14, 2008; in revised form September 6, 2009)

Friction stir welding (FSW) parameters, such as tool material, tool geometry, tilt angle, tool rotational speed, welding speed, and axial force play a major role in the weld quality of titanium alloys. Because of excessive erosion, tool material and geometry play the main roles in FSW of titanium alloys. Therefore, in the present work for the first time, tool material and geometry, tool tilt angle, cooling system and shielding gas effects on macrostructure, microstructure, and mechanical properties of pure titanium weld joint were investigated. Result of this research shows that Ti can be joined by the FSW, using a tool with a shoulder made of tungsten (W) and simple pin made of tungsten carbide (WC). The best conditions for welding were use of compressed air as a cooling system, tool tilt angle of 1°, and a stream of Argon as a shielding medium. Investigation on mechanical properties shows that the tensile strength and the yield strength of the welded joint in the best case could be similar to the corresponding strengths of the base metal.

Keywords friction stir welding, mechanical property, pure titanium, tool material, tool geometry

1. Introduction

Friction stir welding (FSW) is a novel solid-state welding process for joining metals and alloys (Ref 1, 2). Figure 1 shows a schematic illustration of the process. The most important parameters in FSW are the tool material and its configuration and dimensions especially in FSW of high temperature materials such as Ni and Ti. The tool plays three major roles in the formation of the joint: (1) heat the weld zone by friction and plastic deformation, (2) extrude the materials from the front to the rear portion of the pin, and (3) forge the plasticized materials by its shoulder. Titanium usage increases in different industries because of its good corrosion resistance, high temperature resistance, and erosion resistance; therefore, joining of titanium and its alloys become more important. Using traditional fusion welding techniques in joining of titanium develops a brittle cast structure, residual stresses, and undesirable deformation in the welded metals. Thus, using the solid-state welding in order to avoid these problems is necessary (Ref 3). Some investigations have been done on the FSW of Ti alloys (Ref 4-7), but limited attempts have been done on the pure titanium.

Recently, Won et al. (Ref 3) investigated the microstructure FSW of pure titanium. They studied the microstructure and the texture developed from FSW on 5.6 mm thick titanium sheets. They showed that the major mechanism involved in deformation of pure titanium during welding process is twinning. Yu et al. (Ref 8) in the late 2007 studied microstructure and hardness of different areas in the weld formed by FSW on pure titanium.

In the present work, attempts were made to find out the tool geometry, dimensions, material, and tilt angle to have an appropriate transverse speed and the tool rotational speed for forming a joint with higher mechanical properties, while being free of any defect involved in conventional welding processes. In order to achieve such a condition, the macrostructure, microstructure, and mechanical properties of the welded joints made by different test conditions were studied.

2. Experimental Procedure

Titanium as rolled sheet stock of 3 mm thickness was annealed (at 700 °C/1 h) and cut in 140 by 55 mm specimens. Chemical compositions and mechanical properties of the stock material are given in Table 1 and 2, respectively. Four tools with the pin heights of 2.85 mm, pin diameters of 5 mm, and the shoulder diameters of 18 mm were used to make the joints. Based on the tool design and the test condition, experimental tests were carried out in four conditions that have been given in Table 3.

In the test condition number 1, the tool pin and the shoulder were integrated in one piece that was machined from a hardened high-speed steel (HSS) with cylindrical threaded pin profile. In the test condition number 2, the tool consisted of two

K. Reshad Seighalani, Mapna Turbine Blade Engineering and Manufacturing Company (PARTO), Tehran, Iran; **M.K. Besharati Givi**, Department of Mechanical Engineering, University of Tehran, Tehran, Iran; **A.M. Nasiri**, Department of Materials Science and Engineering, Sharif University of Technology, Tehran, Iran; and **P. Bahemmat**, Department of Mechanical Engineering, University of Science and Technology, Tehran, Iran. Contact e-mails: kam.reshad@gmail.com, reshad.kambiz@mapnablade.com, bgivi@ut.ac.ir.

pieces: a threaded cylindrical pin made of tungsten carbide (WC) with a shoulder made of HSS. In the test condition number 3, the tool consisted of two pieces: a simple cylindrical WC pin and a tool shoulder of tungsten (W). The test condition number 4 was same as test condition number 3, except that in this test, a compressed air jet was used as a coolant medium during welding (Table 3). In order to find an improved weld joint, the tilt angle of the tool was changed and the effect of change was investigated. FSW process was carried out with rotational and traverse speeds of 1250 rpm and 3.2 cm/min, respectively, in order to find optimum tool material, design, and tilt angle (conditions 1 to 4II). Then, for improvement of mechanical properties of the weld, the test was done with rotational and traverse speed of 1500 rpm and 6 cm/min, respectively, using a shielding gas (condition 4III).

In order to study macro- and microstructures of the weld, sections of all the specimens were ground, polished, and etched by a solution contained HNO_3 (5 mL), HF (10 mL), and H_2O (80 mL). The specimens were etched 20 s for macrostructure and 7 s for microstructure tests. The etched specimens were studied using optical microscope to investigate quality of the welds and their defects. The tool wear in the weld zone was studied through scanning electron microscopy (SEM). Chemical analysis of worn particles in the weld zone was done using energy dispersive spectroscopy (EDS). Tensile specimens were made by wire electro-discharge machining according to ASTM E8-04 standards. Tensile tests were carried out on a full-automated tensile testing machine with a loading speed of 2 mm/min.

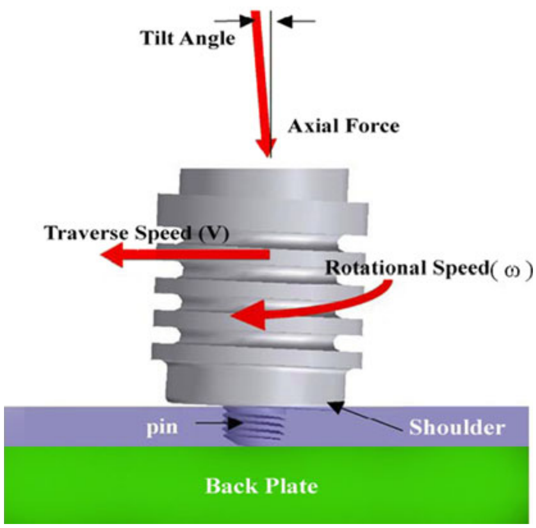

Fig. 1 Schematic illustration of the process

Table 1 Chemical composition of used titanium

Other	Mn	Fe	Al	Ti
Under 0.05	0.05	0.04	0.15	99.7

Table 2 Mechanical properties of annealed titanium

Property	hardness HV, 30 kgf	Elongation, %	US, MPa	YS, MPa
value	148	39	402	342

3. Result and Discussion

3.1 Macrostructure Investigation

Figure 2 shows a cross section of the joint formed under condition 1. The pin height reduced from 2.85 to 1.57 mm during interring to the sheet because of severe wear. Figure 2 shows that penetration of the tool and traverse feeding of the workpiece lead to complete failure of the pin and severe wear of the shoulder nose as a result of heat generated from friction between the tool and the base metal. At the end, the weld became weaker because of complete elimination of the pin and deformation of the shoulder due to severe wearing of the tool during the process. Low-quality weld joint surface and stirred zone (SZ) are shown in the Fig. 2 and 3. Figure 3(a) shows a photograph of the joint surface formed in condition 1. Figure 3(b) shows that the pin completely wore out and dismissed in the tool bottom.

Figure 4(a) shows a cross section of the joint formed under the condition 2 with a tool that consisted of a WC pin and a HSS shoulder. Figure 4(b) shows the material flow of marked zone in the joint cross section in Fig. 4(a), which is inside the stir zone at a higher magnification. The pin geometry in this test was a threaded cylinder with a thread pitch of 0.8 mm. A compressed air jet was used as a coolant medium for cooling down the tool. Surface cracks and impurities in the top part of the weld joint were considerable, and resulted from severe tool shoulder and pin wear in the joint and stir zone. Turbulence and stirring of the materials in SZ caused from friction and plastic work can be seen in Fig. 4(b).

Figure 5 shows the tool shape after finishing the welding process and the joint formed in condition 2. In spite of cooling

Table 3 Test conditions based on tool material and design and cooling system

Test condition	Integration between pin and shoulder	Pin profile	Pin material	Shoulder material	Cooling system	Tilt angle	(ω(rpm), v(cm/min))	Shielding gas
1	Integrated in one piece	Threaded cylinder	HSS	HSS	…	3°	(1250,3.2)	…
2	Integrated in two piece	Threaded cylinder	WC	HSS	Compressed air	3°	(1250,3.2)	…
3	Integrated in two piece	Simple cylinder	WC	W	…	1°	(1250,3.2)	…
4I	Integrated in two piece	Simple cylinder	WC	W	Compressed air	3°	(1250,3.2)	…
4II	Integrated in two piece	Simple cylinder	WC	W	Compressed air	1°	(1250,3.2)	…
4III	Integrated in two piece	Simple cylinder	WC	W	Compressed air	1°	(1500,6)	Argon

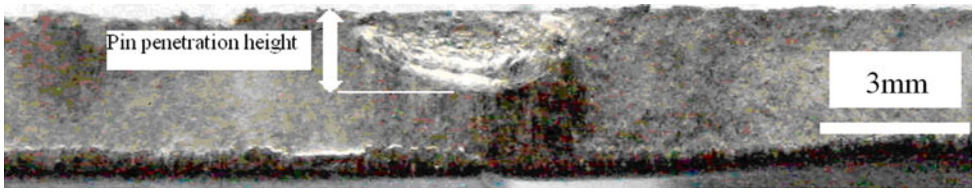

Fig. 2 Macroscopic view of cross-sectional area of the weld joint made under condition 1. Tool penetration is not complete because of severe wear of the tool

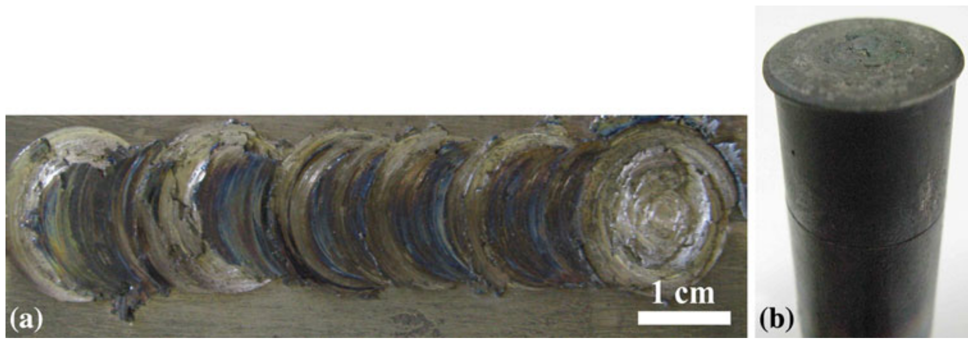

Fig. 3 (a) Photograph made from the joint formed made under condition 1; (b) Used tool made under condition 1 at the end of the FSW

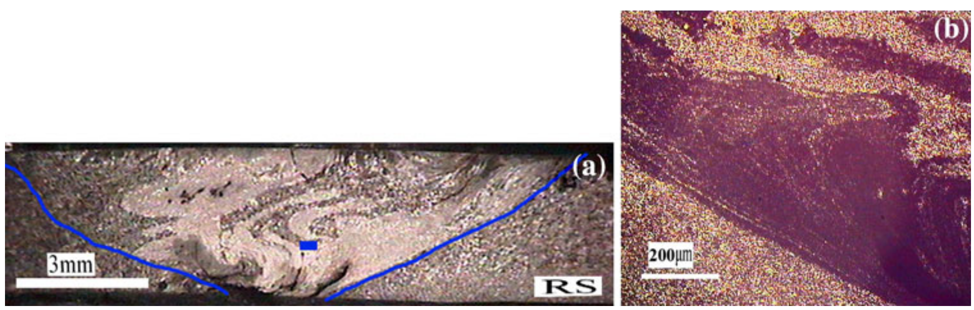

Fig. 4 (a) Macroscopic view of the joint cross section, the joint formed by two pieces; a pin made of tungsten carbide and the shoulder of HSS; (b) Material flow in the marked area

the tool by the compressed air jet, severe tool wear at the end of welding process can be seen clearly. Because stress concentration occurred in the threaded areas, the wear extended to the roots of the threads (Fig. 5b). However, the pin height did not change during welding. Weld surface quality was not good, because the shoulder used was made of HSS (Fig. 5a).

Figure 6(a) shows a cross section of the joint formed under condition 3, with a tool consisting of a WC pin and a W shoulder. The tilt angle of the tool was 1º, and the test was carried out without using any compressed air jet. As shown in Fig. 6(a), some cracks have formed in the top portion of the weld cross section; the cracks caused from the tool shoulder indicate intense wear and penetration of the tool material in the joint area. Different joint zones can be distinguished in this figure. Figure 6(b) shows a rectangular area of Fig. 6(a) at a higher magnification. Material flow in the Stir Zones (SZ) and the linear transition boundary (TB) between the SZ and the HAZ are shown clearly.

Figure 7 shows the effects of changes in the tool tilt angle on the weld joints formed under conditions 4I and 4II. When the tilt angle was 3º, weld surface defects are completely obvious (Fig. 7a). By decreasing the tilt angle to 1º, the surface defects have been dismissed (Fig. 7b).

This phenomenon can be explained by mechanics of FSW process. Friction between the tool and the base metal generates heat, which with rotation of the tool causes severe plastic deformation of material. The weld is created through forging of the deformed material into the cavity that develops behind the tool from the Retreating Side (RS) to the Advancing Side (AS). The gap between the tool and the work piece made from the tilt of the tool expands by increasing the tilt angle. Therefore, by increasing the tilt angle, the plasticized material escapes easily from the bottom of the tool shoulder. Consequently, a discontinuity occurs in the weld, which leads to the formation of some voids at the surface. As can be seen in Fig. 7(a), lack of material in RS and its collection in AS (shown by arrow) show that increasing the tilt angle facilitates removal of the material away from the bottom of the tool. On the other hand, with decreasing tilt angle, forging of the material will not take place; thus the weld will not develop. Therefore, there is an optimum

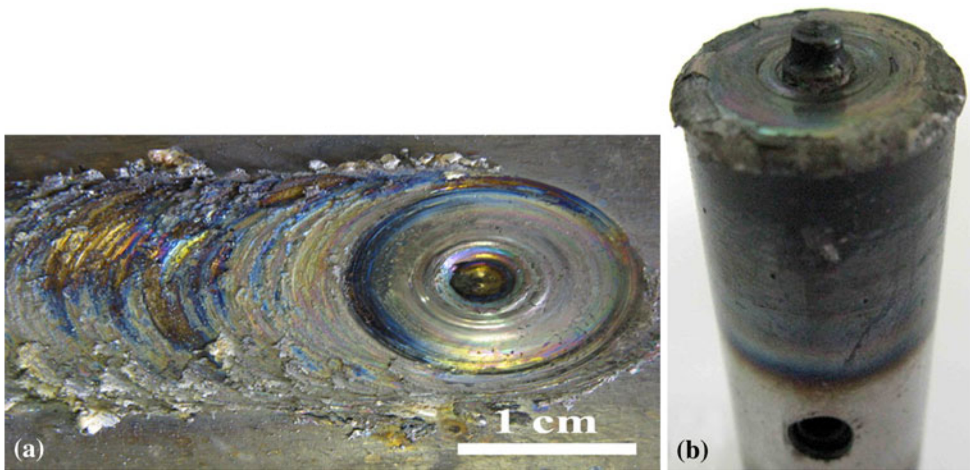

Fig. 5 (a) Photograph of the joint surface formed under the condition 2; (b) Tool under the condition 2 with WC pin and HSS shoulder at the end of FSW process

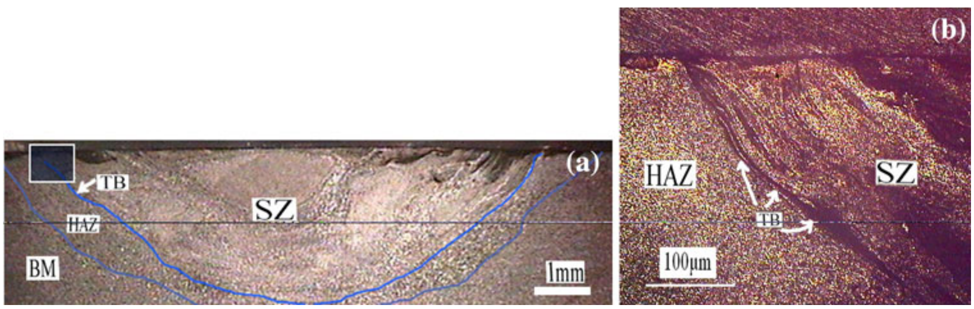

Fig. 6 (a) Photograph made from cross section surface of the joint formed under the condition 3; (b) A photograph made from material flow and structural change in the border between SZ and HAZ

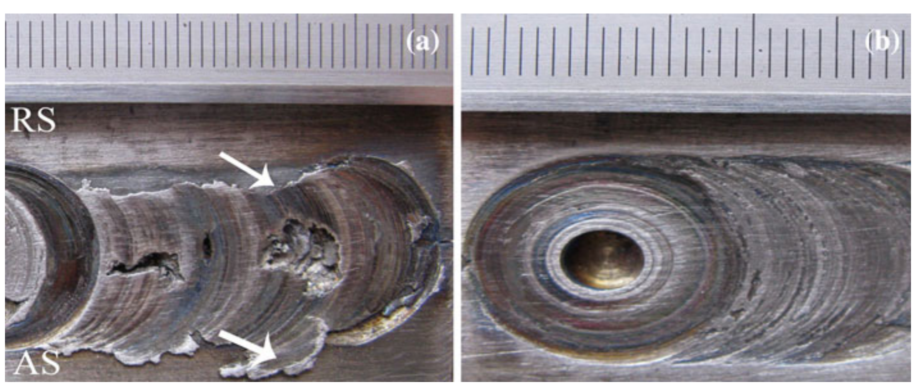

Fig. 7 (a) Voids formed in the joint area under the condition 4I (tilt angle 3º); (b) Joint form under the condition 4II (tilt angle 1º)

value of tilt angle in FSW; which was found to be 1º for pure titanium.

Figure 8 shows a cross section of the joint formed under the condition 4II. In this case, a compressed air jet was used as a coolant and the tilt angle was 1º. These process parameters (cooling system and the tilt angle) have been changed based on previous weld surface quality and tool shoulder wear. Figure 8(a) shows very small cracks under the tool shoulder and fine voids in the weld root; they can be seen clearly in Fig. 9(a). Both of them occurred, because the material had not sufficient fluidity and stirring had not been done properly. So, the rotational and traverse speeds were not optimized. Figure 9(a) shows a cross section of the joint made under condition 4II, in which the tool underwent a little wear, so that tungsten particles as a result of shoulder wear and tungsten carbide particles as a result of pin wear are seen with a maximum size of 20 μm together with a very small amount of titanium oxides (with weight percent of 1.69 for oxygen). Tungsten particles can be observed at the cross section of the joint from surface to the depth of 0.6 mm underneath the

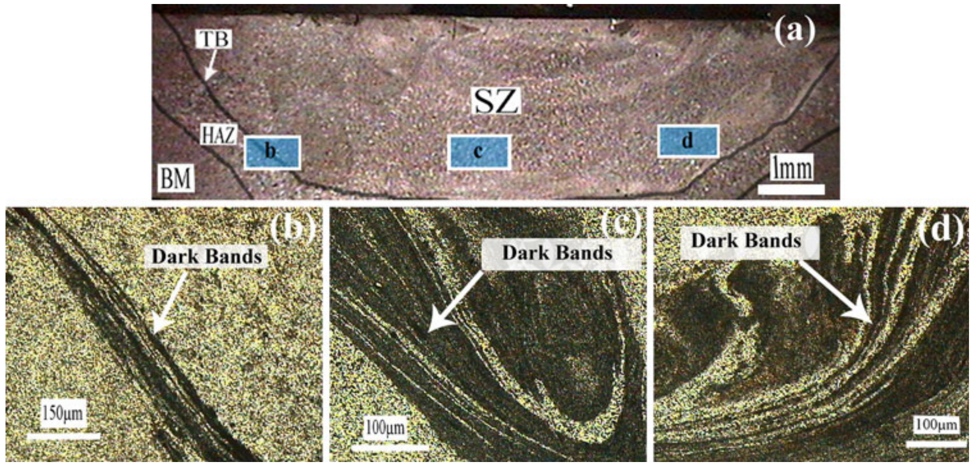

Fig. 8 (a) Transverse cross section of joints formed under the condition 4II; (b) Material flow in TB zone; (c) Material flow feature in the center of the SZ; (d) A photograph made from material flow in the SZ and side of the TB

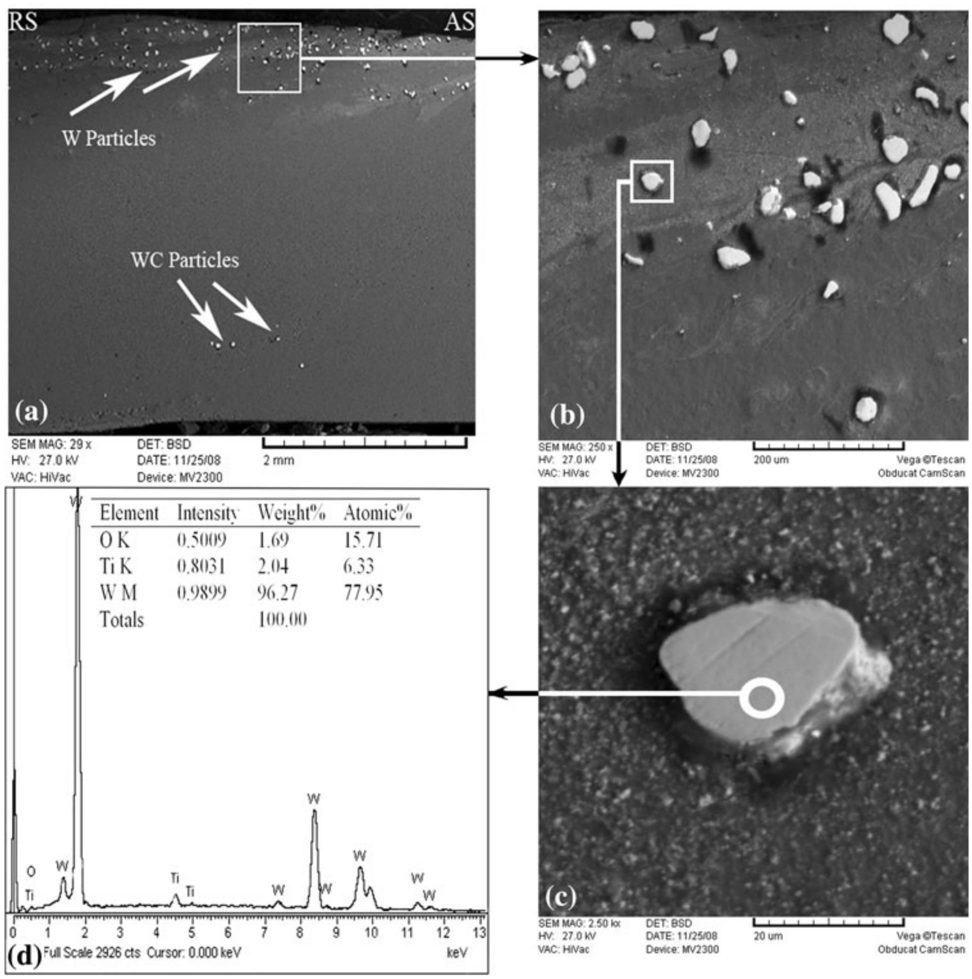

Fig. 9 (a) SEM image taken from cross section of the weld in condition 4II, tungsten particle located in 0.6 mm from tool shoulder and tungsten carbide particles in SZ can be clearly seen; (b) and (c) Magnified view of the pictures a and b, (d) EDS analysis of the particle is shown in c

shoulder (Fig. 9a, 11a). In contrast, tungsten carbide particles are detected just at the middle of the Stirred Zone (SZ). The amount of tungsten particles was much higher than tungsten carbide particles, which indicates that tungsten carbide has more resistance for severe wearing during the FSW process than tungsten.

Small amount of titanium oxide (with weight percent of 1.69 for oxygen) are developed because of high reaction between titanium and oxygen and lack of shielding gas protection of the weld. As can be seen from the figure, wear of the tool pin is very small. Figure 9(b) and (c) demonstrates higher magnification of Fig. 9(a). Figure 9(d) shows an EDS analysis of wear particles accommodated in the bottom of the joint.

Macroscopic views of the joint cross section made under the condition 4III (Fig. 10, 11) shows that the weld in the region is free of any kind of welding defect. EDS analysis of a random point selected from the substrate in the SZ shows that there is no titanium oxide in the zone; this is because of protection of argon gas used as a shielding gas. Figure 12 shows the top and rear views of the joint and the tool used for condition 4III.

Fig. 10 Macroscopic view of the joint cross section in condition 4III

However, study of the weld macrostructure shows that, the first and the most fundamental step to achieve a defect-free weld joint is using a tool with a correct material and geometry and then optimization of the rotational and travel speeds. Because rotational and traverse speeds play the most important role in flow and efficient stirring of the material plasticized through friction and plastic work (Ref 9), using a two-piece tool consisting of a WC pin and a shoulder of W, together with compressed air jet as a coolant and Argon as a shielding gas can achieve a weld joint free of any weld defect.

Investigation of the defect-free joint microstructure shows that there are three distinct zones: (1) Stir Zone, (2) Heat Affected Zone, and (3) a narrow Transition Boundary (TB). In fact, in the joining of pure titanium compared to aluminum and its alloys, thermo-mechanically affected zone (TMAZ) does not develop (Ref 1, 10, 11). In Fig. 8(b) and 6(b) the linear TB can be seen clearly. Therefore, the changes in grain size and elimination of the dark bands in TB happen very quickly in a very thin band.

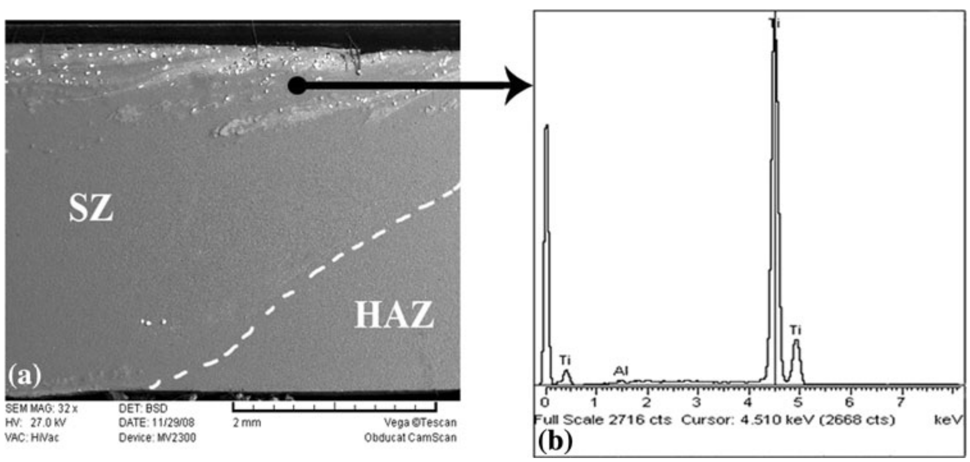

Fig. 11 (a) SEM view of the joint cross-sectional area developed in condition 4III, showing small wear of the tool shoulder and having joint free of metallurgical defect. (b) EDS analysis of the point shown in Fig. 11(a); it shows that there is no oxidation of titanium occurred because of using argon as shielding gas

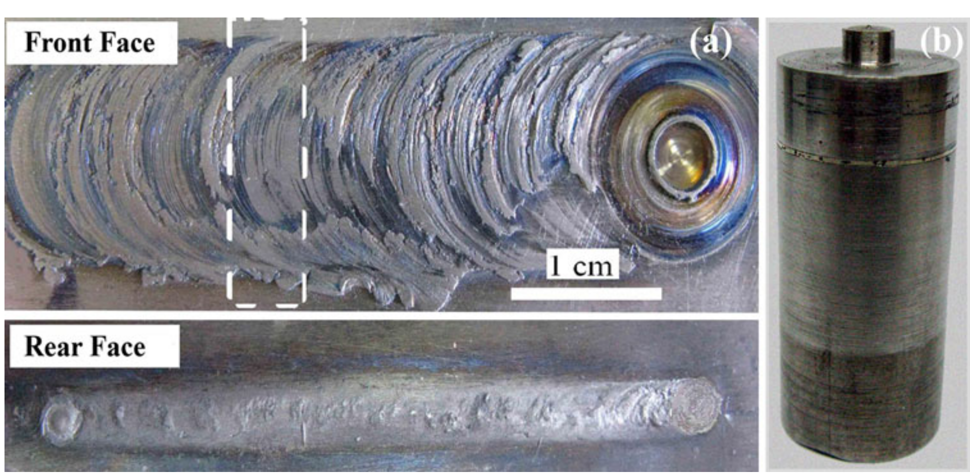

Fig. 12 (a) Joint formed by condition 4III with the tilt angle of 1º; (b) Used tool in condition 4III after FSW

3.2 Investigation of Mechanical Properties

Tensile strength, yield strength, and elongation of the joints formed under all the four conditions are given in Fig. 13. As shown in Fig. 13, the highest tensile strength and yield strength are related to condition 4III, in which a two-piece tool (consisting of a pin of tungsten carbide and a shoulder of tungsten) with a compressed air jet as a coolant for cooling the tool have been used. In this condition, titanium oxide formation has been prevented by using argon gas jet as a shielding gas. The tensile strength and yield strength of the joint are 402 and 341.15 MPa, respectively, and are comparable to the values for the base metal. Figure 14 shows the tensile specimens in condition 4III after the tension test in which fracture occurred 17 mm away from the center of the joint. Necking (pointed by arrows in the figure) happened in the RS of the specimen. Location of the specimen cut from the joint has been shown by the broken lines in Fig. 12(a). Total elongation of the specimen is 25.7% which is 13.3% lower than that of base metal (39%). The reason for this reduction in elongation is that the tensile specimen was cut in the transverse direction to the weld axis and the gauge length (subjected to a constant load) elongated with different amounts of local strains in different zones. However, the HAZ and the base metal were subjected to plastic deformation that led to necking of the specimen; but the SZ region was not necked, because its ultimate strength was higher compared with the other regions in the specimen. Increased ultimate and yield strengths of the joint made under the condition 4III are because of a decrease in the grain size of the SZ.

The ultimate strength and the yield strength of the joint obtained under the condition 4II are 87 and 92% of corresponding values of the base metal. Fracture of the tensile specimen of the joint made under the condition 4II, occurred in the weld zone; this is due to the voids formed in the weld root and the titanium oxide developed through the joint surface (can be seen in the SEM image of Fig. 9a). In other words, with optimized rotational speed that can eliminate the defects developed in condition 4III and improved uniformity of the weld structure, the fracture point moves from the weld zone to the base metal (condition 4III).

4. Conclusions

1. Using high-speed steel (HSS) tool for FSW of titanium will result in complete failure of the pin and severe wear of the shoulder nose because of heat generation from friction between the tool and the base metal.
2. Using brittle WC as a pin material for FSW of the Ti-CP and because of high wear and stress concentrations developing on the root of the pin's threads during this process, these threads were eliminated.
3. Macrostructural analysis of the welded joints shows that FSW of pure titanium under the test condition 4III that consisted of a simple cylindrical WC pin and a W shoulder, together with the application of compressed air jet as a coolant, Argon as a shielding gas, and a tilt angle of 1º for the tool can lead to a defect-free weld joint.
4. According to the microstructural investigation of FSWed CP-Ti, next to the WN, there exists a linear transition

Fig. 14 The tensile specimen of condition 4III after tension test, fracture occurred in 17 mm away from the center of joint, necking (pointed by arrows) was happened in RS of the specimen as well

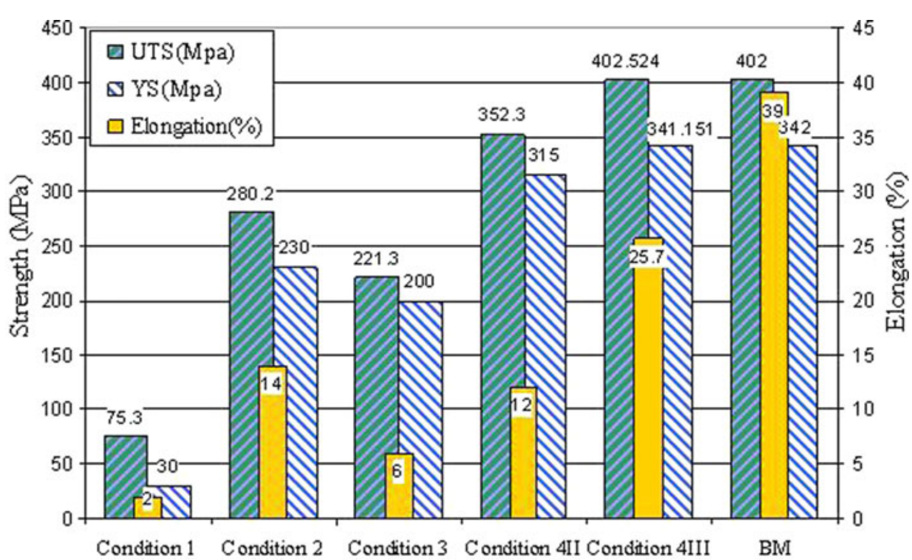

Fig. 13 Comparison of mechanical properties in five cases

boundary (TB) situated between the WN and the HAZ and no TMAZ was detected.
5. Data obtained from tensile tests of the specimens cut from the transverse directions of the weld joints show that the tensile and the yield strengths were highest for the joint made by tool 4 because there was no weld defects such as void or impurity in the weld surface and the cross sections.
6. The present research shows that FSW with a tool made of two pieces can be successfully used to join pure titanium sheets.

References

1. R.S. Mishra and Z.Y. Ma, Friction Stir Welding and Processing, *Mater. Sci. Eng. Rep.*, 2005, **R50**, p 1–78
2. W.M. Thomas and E.D. Nicholas, Friction Stir Welding for the Transportation Industries, *Mater. Design*, 1997, **18**, p 269–273
3. W. Lee, C.Y. Lee, W. Chang, Y. Yeon, and S. Jung, Microstructural Investigation of Friction Stir Welded Pure Titanium, *Mater. Lett.*, 2005, **59**(26), p 3315–3318
4. D.G. Sanders, M. Ramulu, E.J. Klock-McCook, P.D. Edwards, A.P. Reynolds, and T. Trapp, Characterization of Super Plastically Formed Friction Stir Weld in Titanium 6Al-4V: Preliminary Results, *JMEPEG*, 2008, **17**, p 187–192
5. Y. Zhang, Y.S. Sato, and H. Kokawa, Microstructural Characteristics and Mechanical Properties of Ti-6Al-4V Friction Stir Welds, *Mater. Sci. Eng. A*, 2008, **485**, p 448–455
6. R. John, K.V. Jata, and K. Sadananda, Residual Stress Effects on Near-Threshold Fatigue Crack Growth in Friction Stir Welds in Aerospace Alloys, *Int. J. Fatigue*, 2003, **25**, p 939–948
7. A.L. Pilchak, M.C. Juhas, and J.C. Williams, Microstructural Changes due to Friction Stir Processing of Investment-Cast Ti-6Al-4V, *Metal. Mater. Trans. A*, 2007, **38A**, p 401–408
8. Y. Zhang, Y.S. Sato, H. Kokawa, S.H.C. Park, and S. Hirano, Stir Zone Microstructure of Commercial Purity Titanium Friction Stir Welded Using pcBN Tool, *Mater. Sci. Eng. A*, 2008, **488**, p 25–30
9. M. Pareek, A. Polar, F. Rumiche, and J.E. Indacochea, Metallurgical Evaluation of AZ31B–H24 Magnesium Alloy Fiction Stir Welds, *JMEPEG*, 2007, **16**, p 655–662
10. S. Lomolinoa, R. Tovob, and J. dos Santos, On the Fatigue Behavior and Design Curves of Friction Stir Butt-Welded Al Alloys, *Int. J. Fatigue*, 2005, **27**, p 305–316
11. K. Elangovan and V. Balasubramanian, Effect of Pin Profile and Rotational Speed of the Tool on the Formation of Friction Stir Processing Zone in AA6061 Aluminum Alloy, *J. Mater. Manuf. Process.*, 2008, **23**(3), p 251–260